Chemical free lysis and fractionation of cells using surface acoustic waves for sensitive protein assays.

Ali Salehi-Reyhani,*[a] Frank Gesellchen,[†b] Dileep Mampallil,[†b] Rab Wilson,[b] Julien Reboud,[b] Oscar Ces,[a,c] Keith R. Willison,[a,c] Jonathan M. Cooper*[b] & David R. Klug*[a,c]

[a] Proxomics, Institute of Chemical Biology, Imperial College London, London, SW7 2AZ (UK)

[b] Division of Biomedical Engineering, School of Engineering, University of Glasgow, Oakfield Avenue, Glasgow G12 8LT (UK)

[c] Institute of Chemical Biology, Department of Chemistry, Imperial College London, London, SW7 2AZ (UK)

ABSTRACT: We exploit the mechanical action of surface acoustic waves (SAW) to differentially lyse human cancer cells in a chemical-free manner. The extent to which cells were disrupted is reported for a range of SAW parameters and we show that the presence of 10μm polystyrene beads is required to fully rupture cells and their nuclei. We show that SAW is capable of subcellular fractionation through the chemical-free isolation of nuclei from whole cells. The concentration of protein was assessed in lysates with a sensitive microfluidic antibody capture (MAC) chip. An antibody-based sandwich assay in a microfluidic microarray format was used to detect unlabelled human tumour suppressor protein p53 in crude lysates, without any purification step, with single molecule resolution. The results are digital, enabling sensitive quantification of proteins with a dynamic range >4 orders of magnitude. For the conditions used, the efficiency of SAW-induced mechanical lysis was determined to be 12.9 ± 0.7% of that for conventional detergent-based lysis in yielding detectable protein. A range of possible loss mechanisms that could lead to the drop in protein yield are discussed. Our results show that the methods described here are amenable to an integrated point-of-care device for the assessment of tumour protein expression in fine needle aspirate biopsies.

Fine Needle Aspiration is a standard clinical tissue sampling technique used widely as a biopsy for a range of conditions, in particular to see whether a palpable or imaged tissue mass is malignant. The procedure produces fine needle aspirates (FNAs) which typically contain a few 100,000 loosely connected cells from the sampled tissue. These are currently analysed for malignancy using standard histological methods. There is increasing interest in obtaining more detailed phenotypic and genotypic information for the purposes of improved disease management for the benefit of the patient as well as research into human cancer biology. For example, a recent study using multiple FNAs from the same and different tumours in a single patient showed that not only were the tumours heterogeneous but that the tissue within each tumour showed a level of heterogeneity far greater than had previously been expected.[1]

For many cancers, diagnosis of malignancy is a time-critical process. The sooner a tissue can be identified as cancerous the greater the chances of effecting successful treatment. It may therefore be extremely beneficial to both patient and clinic if diagnosis could be made while the patient is in attendance and subsequent clinical actions scheduled accordingly.

In order to achieve this point-of-care diagnostic response, it is necessary to develop devices capable of phenotyping and/or genotyping an FNA sample directly from the needle itself such that the needle need only be inserted into the instrument to obtain an initial diagnosis. To do this, the instrument needs to be able to lyse the cells and read out the markers of choice, be they genes or proteins.

Direct analysis of FNA material from the needle without performing chemical extraction has been demonstrated using direct needle spray ionisation mass spectrometry.[2] While mass spectrometric analysis in a clinical setting has been reported,[3] the cost and complexity of these instruments make their wide spread use for routine diagnoses unlikely in the short term. Microfluidic chip based technologies would seem to be more suitable for this purpose as it is possible to integrate a range of processes into single devices, which can be both cheap to pro uce and easy to use. To demonstrate the potential capabilities of such devices in the context of phenotyping FNA material we integrate a Surface Acoustic Wave (SAW) lysis method with a Microfluidic Antibody Capture (MAC) protocol capa ble of single molecule readout of proteins.

The mechanical manipulation of fluids afforded by surface acoustic waves (SAWs) enables a range of different applica tions;[4,5] such as the mixing and movement of material in sur face droplets and microfluidic channels,[6] the concentration of particles,[7–9] the nebulisation of samples for mass spectrome try,[10] rapid chip based fluorescence activated cell sorting,[11] investigation of cell adhesion with techniques such as cell pealing,[12,13] along with SAW induced mechanical lysis of cells, which is due to the acoustic streaming effect.[14–16] When a SAW meets a water based droplet, it refracts into the liquid and induces flow within the confined droplet. If the droplet is exposed to SAW along a fraction of its width, a vortex is es

tablished.[8] The shearing forces due to the rotational fluid mo $ion within the droplet acts to disrupt cell membranes, leading to cell lysis. SAW has previously been integrated with PCR as a single platform to perform chemical ,ree lysis and detection of malarial parasites in blood with a sensitivity similar to that of lab based PCR tests.[15] Together with a recent report of sim ple methods to generate SAW using aluminum foil electrodes, this demonstrates the potential of SAW for low cost point of care applications.[17]

While genomic and transcriptomic studies provide powerful insights, only weak correlations between mRNA and protein expression have been found.[18,19] As the transcriptome is in some cases only a partial reflection of the functional status of a cell, tools and techniques to measure proteins are needed to fully understand cell function. Several microfluidic based approaches to perform sensitive protein measurements have been reported.[1,20–22]

We have developed a Microfluidic Antibody Capture (MAC) chip that is capable of performing sensitive protein measurements on single cells.[20] Using optical tweezers, the platform manipulates and isolates single cells into nanolitre sized analysis chambers where they are individually lysed by laser induced microcavitation. The contents of the cell are released and diffuse freely in the chamber. Specific proteins, and protein complexes, can be captured and detected with an antibody sandwich system using two antibodies binding to different epitopes on the target. The capture antibody is mi croarrayed as ~100µm spots onto a functionalised coverslip, which also seals the device. The capture antibody binds the protein of interest at the surface, and a fluorophore labelled detection antibody then binds to the captured protein in a sandwich configuration. Binding is detected using total inter nal reflection fluorescence (TIRF) and a sensitive camera, a system enabling single molecule detection, so that individual binding event may be counted. The MAC chip platform is able to determine the absolute number of proteins within a single cell and confers high precision, accuracy and dynamic range on the overall results.[23,24] Promising efforts by other groups have demonstrated low cost, yet highly capable, fluorescence microscopy on chip solutions[25,26] as well as inexpensive TIRF.[27]

Here we adapt the method to measure specific protein con centration in a cell lysate obtained using SAW. In principle, the combination of SAW and MAC technology produces a tool which is of the highest possible sensitivity and is quantita $ive, yet which could be automated and deskilled sufficiently to allow a nurse or technician to insert the FNA into the device and retrieve the readout. It is attractive to produce lysate using the mechanical forces of SAW since cells may be maintained in physiological buffer up until the point of lysis. This helps proteins and protein complexes to remain in their native forms for downstream protein assays. Furthermore, it requires no reagents other than the cell suspension itself to produce the lysate.

This paper demonstrates that SAW and MAC technology have the requisite capabilities to be combined for the purpose of FNA analysis. The rapid, sensitive readouts produced show potential for the application of the technique at the point of care.

METHODS & MATERIALS

Overview of Experimental Procedure. We obtained ly sates using the SAW lysis method and measured the concen tration of protein directly from the crude lysates using the MAC chip. Droplets of cell suspensions were pipetted onto the SAW device, which upon actuation created a vortex within the droplet, resulting in cell lysis. 20 µL droplets of cells con taining 2×10^4 cells were used to resemble fine needle aspirate samples.

The lysate produced by SAW was then transferred into a MAC chip with a geometry suitable for testing the lysate. The performance of SAW was compared by carrying out the same assay but producing the lysate with conventional detergent based lysis buffers instead. SAW lysis was also assessed by imaging cell suspensions before and after the application of SAW.

The protein of interest, p53, was captured by the antibody spots in each analysis chamber of the MAC chip and binding was detected using TIRF microscopy and monitored over time. The acquired images were processed automatically to determine the number of single molecules bound to the anti body spot at equilibrium. The details of the process are de scribed below.

Cell Culture and Preparation. The BE human colon car cinoma cell line has previously been shown to exhibit high p53 protein expression.[23]

BE cells are cultured using Dulbecco's Modified Eagles Medium (DMEM; Invitrogen, UK) supplemented with 10% (v/v) foetal bovine serum (FBS; Sigma, UK) in a cell incuba tor.

Cells used in experiments were detached from culture flasks using Accutase (Sigma, UK), which was inactivated by sus pension in culture medium. The suspension of cells was gen tly agitated with a P1000 pipette (Eppendorf) to produce a single cell suspension. Cells were then centrifuged at 200g for 5 min. at 4°C. The supernatant was replaced with ice cold phosphate buffered saline (PBS) and cells counted using a haemocytometer.

SAW Platform. The experimental setup is shown in **figure 1a**. The sample to be lysed is deposited on a phononic super strate which sits on a lithium niobate ($LiNbO_3$) piezoelectric wafer supported by a metal heat sink. The asymmetric acous tic field induces a vortex in the droplet sample which leads to mechanical cell lysis (**figure 1b**). We have previously reported the methods used here and these are reproduced in part below.[15]

Lithium Niobate wafer fabrication. SAWs were generated by a piezoelectric 128° Y cut X propagating 3 in $LiNbO_3$ wa fers. The devices consisted of 20 pairs of electrodes to form an interdigitated transducer (IDT) with a pitch of 200 µm, width of 100 µm, and an aperture of 10 mm, yielding a frequency of approximately 10 MHz for the propagating SAW. Frequencies with which vortices were achieved in the droplet varied be tween 9.7 and 10.3 MHz.

Phononic crystal superstrate design and fabrication. The phononic superstrate comprises a square array (pitch 203µm) of circular holes (radius 82 µm) in a 470 µm thick silicon wa fer that scattered the SAW to obtain an asymmetry in the acoustic field. An area of 5 mm in diameter on the surface of the superstrate was made hydrophilic at the location where the sample droplet would be located. The rest of the surface was

made hydrophobic by a 1.6 mM silane (trideca-fluoro-l,l,2,2-tetrahydrooctyltrichlorosilane; Sigma, Europe) solution in heptane (Sigma, H9629) applied for 5 min.

SAW Platform. The IDT was connected to an MXG Analog Signal Generator N5181A (Agilent Technologies) in conjunction with a Mini Circuits ZHL-5W-1, 5–500 MHz amplifier. The procedure was observed under a stereomicroscope.

The superstrate was placed on top of the piezoelectric wafer and coupled with 2 μL of water-based gel (KY Jelly; Johnson and Johnson) spread manually in between, yielding a film approximately 50-μm thick.

MAC Chip Platform. Here we use the MAC chip methodology for the sensitive detection of a specific protein in crude lysates (**figure 2**).

Antibodies. Tumour suppressor p53 protein was detected using an antibody sandwich assay. The anti-p53 capture antibody was taken from a commercial test kit (p53/Mdm2; Enzo Life Sciences, UK) and the detection antibody is the DO1 clone anti-p53 monoclonal antibody fluorescently labelled with Alexa Fluor 488 (Santa Cruz, Europe).

Microarray fabrication. Capture antibody spots were printed onto Nexterion coverslips (Schott, Europe) using an OmniGrid Micro microarrayer (Digilab, UK) and a 946MP2 pin (ArrayIt, USA). The spotting solution contained anti-p53 capture antibody mixed 1:1 with a print buffer comprising 3×SSC, 1.5M betaine supplemented with 0.01% SDS; the final concentration of anti-p53 in the spotting solution was 0.5 mg mL^{-1}. Spots were printed at defined coordinates in a regular array which filled the area of a 65 × 25 mm coverslip using the AxSys microarray software. The printed coverslips were stored at 4°C before use.

Microfluidic device fabrication. PDMS channels were fabricated using SU-8-based soft-lithography techniques. The analysis chambers were cylindrical with a radius and height of 250μm and 50μm, respectively. PDMS was mixed at a ratio of 10:1 precursor to curing agent and poured over the SU-8 mould before being degassed in a desiccator chamber and set to cure at room temperature for 24+ hours. The cured PDMS was removed from the mould and 300 μm access holes were drilled (Diama, UK) at the end of each channel. The PDMS was exposed to air plasma for 1 minute before the microchannels were sealed by a coverslip upon which antibody spot arrays had been printed in defined locations. The antibody microspots were aligned into the analysis chambers using a home built translation stage. The bonded device was stored in a fridge at 4 °C in a sealed chamber overnight before use.

Producing Cell Lysate. *Detergent-based lysis.* As a control, lysate was produced using detergent. Cells were detached and prepared as above. The concentration of cells was adjusted to 2×10^6 cells/mL before being mixed with an equal volume of RIPA lysis buffer supplemented with a cocktail of protease inhibitors (Sigma, Europe). The lysate was not fractionated and the entire lysate was used as produced.

SAW-induced mechanical lysis. Cells were stored in 1mL Eppendorf vials and placed on ice. The vial was briefly mixed to homogenise the cell suspension prior to pipetting 20μL droplets onto the phononic superstrate. The SAW device was powered on at 10 ± 0.3 MHz for 30s during which cells would lyse (**figure 1c**). The droplet was harvested by pipetting and stored in an Eppendorf tube placed on ice. Approximately 200μL of lysate was accumulated by successive lysis and harvesting of 10 droplets of cells.

SAW-induced mechanical lysis, or simply SAW lysis, was also performed on droplets of cells containing an equal concentration of beads. Monodisperse 10μm diameter polystyrene beads (Sigma, Europe) were washed to remove additives by centrifugation in PBS and stored at 4°C at a concentration of 1×10^7 beads/mL before use.

Testing Cell Lysate with MAC Chips. *Platform*. An inverted microscope (Nikon Ti-E, Nikon, Japan) was used as the experimental platform. Antibody spots are imaged automatically in series by objective-based total internal reflection fluorescence (TIRF) microscopy at λ = 488 nm and 1.5 mW. TIRF illumination only excites fluorophores within ~100nm of the surface so the focal plane was maintained by a Nikon Perfect Focus System (Nikon, Japan). The use of an electron-multiplied CCD camera (IXON DU-897E; Andor Technologies, Ireland) enables single molecule detection sensitivity. The accumulation of fluorescence indicates the binding of p53 bound to anti-p53 labelled detection antibody to the surface antibody spot.

Procedure. Immediately before use, each MAC chip was removed from the fridge and equilibrated to room temperature. The chip was secured on the microscope's encoded XY stage and the position of all antibody spots recorded in addition to two points on the chip, which were used as fiducial markers. The device was removed from the microscope and the input and output reservoirs filled with 4% PBSA (PBS supplemented with 4% (w/v) bovine serum albumin) before being placed in a desiccator. After degassing the devices were filled with 4% PBSA which serves to block the antibody spot and microfluidic channels from non-specific binding of protein. The chip was then returned to the microscope and connected via appropriate tubing to syringe pumps (Labsmith, USA). Since the antibody spots were no longer visible, the fiducial markers were used by a simple Matlab script to correct the positions of the antibody spots. Fluid flow in each lane was controlled individually using separate syringe pumps. To replace the solution in each channel, the syringe pumps drew 5μL of fluid from individual sample reservoirs at 5μL min^{-1}.

Image acquisition. The EM-CCD camera settings were as follows; 900ms acquisition time, electron multiplier gain 10 and the readout mode set to 1MHz at 16-bit. Each spot was imaged in series every 10min for 30min then every 20min for a further 60min.

Data analysis. Once data was acquired, single molecules were detected by identifying 4-9 clustered pixels, with circularity greater than 0.5 and with pixel intensities at least 3 times the background standard deviation plus its mean value. When protein copy number is high, bound proteins become congested and the single molecule images overlap and are individually indistinguishable. In this regime, the number of proteins captured can be estimated from dividing the antibody spot intensity by the known average intensity of a single molecule. All data analysis to determine the number of single molecules bound to an antibody spot was automated using algorithms written for FiJi.[28]

Immunofluorescence. *Immunostaining of fixed cells.* BE cells were fixed, permeabilised, then immunostained following methods described in Stadler *et al*.[29] Cells were grown upon

22mm × 22mm No. 1.5 thickness glass coverslips placed in the wells of a 6 well plate. At ~80% confluence cells were removed from the incubator and washed 3× with ice cold PBS. For fixation, cells were treated with freshly made ice cold 4% paraformaldehyde in cell growth media then washed 3× with PBS. Cells were permeabilised using 0.1% (w/v) Triton X 100 and an exposure of 15min, replacing the solution every 5min. Cells were incubated overnight at 4ºC with 1µg mL^{1} anti p53 antibody (DO 1; Santa Cruz, Europe) labelled with Alexa Fluor 488 in 4% PBSA. After washing 4× with ice cold PBS for 10min, cell nuclei were stained with 300nM DAPI in PBS and washed again 4× with ice cold PBS for 10min. Wells were filled with 78% glycerol in PBS, sealed and stored at 4ºC before image acquisition.

Image acquisition. Widefield fluorescence was performed on the same inverted microscope using a mercury lamp (Nikon, Japan). In addition to the TIRF filter set (Chroma, USA), standard DAPI and FITC filter sets (Nikon, Japan) were used. The coverslips upon which cells were grown was mounted on a homemade mount. Although cells could just as straightforwardly been grown directly on the plastic surface of a well plate, coverslips permit high resolution fluorescence microscopy. Images were acquired and analysed using the NIS Elements software (Nikon, Japan).

RESULTS & DISCUSSION

Testing cell lysate with MAC Chips. The variant of the MAC chip which was used possessed 5 lanes per chip with 15 analysis chambers per lane and enabled 5 different lysate solutions to be tested in parallel. This by no means represents a technical limit per chip and was simply designed to be adequate for our purposes here.

Figure 2b shows typical raw images which are used by the single molecule counting algorithms to determine the number of p53 proteins bound to the antibody spot under different conditions.

Before flowing in lysate test solution, spots are first incubated for 30min in solution containing only 0.25µg mL^{1} anti p53 Alexa Fluor 488 labelled detection antibody in 4% PBSA. This gives a low non specific background count on the spot and single molecules were spatially well separated. Their individual intensities were easily measured and helped in determining the average fluorescence intensity of the single molecules.

Cell lysates are complex mixtures containing thousands of different proteins. As is often the case, protocols to produce lysate specify that the lysate is spun down to remove cell debris such as membrane and DNA. After performing SAW lysis it is desirable that we avoid processing the lysate further such as by centrifugation or purification. However, this could potentially be problematic to the p53 assay due to various mechanisms by which species could non specifically bind to the capture antibody spot and interfere with the readout.

Non specific binding (NSB) of proteins can potentially mislead results unless the assay is well characterized and understood. We performed separate assay validation experiments to test the specificity of the p53 assay for p53 protein. **Figure 2c** summarizes the controls that have been made along with the corresponding single molecule counts for each control. The greater than 10^{4}–fold increase in single molecule counts when comparing the complete antibody sandwich clearly shows that the assay is sufficiently robust and specific to p53 even in crude cell lysate.

SAW lysis and subcellular fractionation of cells. The activity of p53 depends on, among other factors, its subcellular localisation.[30] In normal cells under non stressed conditions, p53 shuttles between the nucleus and the cytoplasm and is expressed at low levels.[31,32] In response to stress, p53 is post translationally modified which results in its accumulation in the nucleus.[32]

BE cells were imaged using fluorescence microscopy to determine the subcellular localisation of p53. **Figure 3** presents representative images of BE cells immunostained with labelled anti p53, showing predominantly a localisation within the nucleus.

The extent to which BE cells were lysed using SAW was then determined by pipetting the droplet of lysed cells from the phononic superstrate onto a microscope coverslip and by fluorescence imaging (**figure 4**). To help in evaluating SAW lysis, the cell permeant fluorescent DNA stain Hoechst 33342 and Calcein AM were used to stain cell nuclei and cytoplasm prior to lysis. Calcein AM is non fluorescent but is converted to a green fluorescent product after hydrolysis by intracellular esterases and indicates that the cell is viable.

As expected, when applying SAW without vortex formation all cells remained intact; their morphologies were round with rounded nuclei (**figure 4a**). When a vortex was applied only a few cells remain fully intact as observed by the green fluorescence of Calcein AM, whereas most nuclei remain intact, or the DNA remains compacted, as observed by the blue fluorescence of the Hoechst dye (**figure 4b**). Since the lysis effect of SAW is due to shear stress within streaming flows, which are dependent on SAW amplitude, the output power of the signal generator was increased. Increasing the applied power from 0.8W (8 Bm at signal generator) to 2W (4 Bm) improved the number of cells with a disrupted cytoplasm; however the nuclei were still able to withstand the increased shear stress (**figure 4c**). Power was ramped further but several detrimental effects were observed at higher powers. Firstly, the droplet evaporation rate rose significantly and secondly, nebulisation of the droplet began to occur. SAW induced nebulisation has been used effectively to nebulise non volatile analytes for mass spectrometric analysis.[33] Here nebulisation is not desirable since it represents a source of material loss. Furthermore, the higher energy input into the phononic superstrate may result in sufficiently raising the temperature of the droplet to start to denature proteins.

In an effort to further improve efficiency, without increasing power, 10µm polystyrene beads were spiked into the suspension of cells. In the droplets cells and beads were both present at an equal concentration of 1×10^{6} beads or cells/mL. With input power set to 8 Bm and beads present, the cell membranes are almost completely disrupted by SAW lysis but nuclei appeared to remain intact; although some displayed a jagged and shrivelled appearance (**figure 4d**). When input power was increased to 4 Bm with beads present, cell nuclei were predominantly disrupted with a few remaining intact (**figure 4e**). Nuclear debris, as determined by blue Hoechst fluorescence, is observed to be elongated suggesting they underwent shearing.

It is unclear exactly how beads aid SAW lysis.[16] The density of the beads is ~1.05g cm^{3} which is similar to cell density,[34] suggesting the rigidity of the beads may play a role in improv ing lysis efficiency. Due to their similar diameter to the BE cells, it is unlikely for the beads to reach higher velocities than cells, which could contribute to a higher shearing force. It is possible that the action of the beads is such that when two or more beads come in contact with any cells they act to deform and grind them.

Efforts were made to improve lysis efficiency by increasing vortex time from 30s up to 2min but no significant differences were observed suggesting that any lysis produced by SAW has completed within 30s, which is in agreement with previously published data.[15] Droplet volume was also altered while main taining the number of cells and beads constant (2×10^4/droplet). The droplet volumes tested were 10µL, 50µL and 100µL and did not improve SAW lysis efficiency. Of course, increasing droplet volume would have the undesirable effect of reducing cell concentration and therefore lysate concentration. Howev er, it was thought that the increase in tangential speed of cells as they stream from the edge of the larger droplets to the cen tre during SAW lysis may have compensated by increasing overall lysis efficiency. However, the desired effect was una ble to be tested since vortices were harder to achieve in the larger droplet volumes.

Standard protocols to isolate nuclei from mammalian cells involve hypotonic swelling and the use of, albeit gentle, deter gents. The results presented here indicate that SAW may be a tuneable mechanism for cell lysis, with the potential to isolat ing cell nuclei in a chemical free fashion. Subcellular fraction ation techniques have been widely used to investigate the structure and function of organelles as well as to study the location and intracellular dynamics of various molecules.[35,36]

Testing cell lysate produced with SAW lysis. To test the potential to integrate SAW induced mechanical lysis to release intracellular proteins, post SAW lysis detection of p53 protein was performed using the 5 lane flow style MAC chip (**figure 2a**).

In order for optimal detection of p53 protein to be made, both cells and their nuclei must be disrupted. Therefore, BE cell lysate was produced using SAW with 10µm beads spiked into the suspension of cells. A 20µL droplet was pipetted onto the phononic superstrate and vortexed for 30s before being harvested by pipette. The lysate was pipetted up and down several times over the droplet to mix the suspension and col lect as much material from the surface as possible. SAW ly sate was immediately transferred to an Eppendorf placed on ice. Approximately, 200µL of lysate was accumulated by suc cessive lysis of 10 droplets.

The addition of beads has been shown to improve the extent to which cells are disrupted. However, polymer beads are generally hydrophobic so have a high protein binding capacity therefore steps to block non specific binding were made. Beads were either blocked using a solution of 4% PBSA or 0.05% Tween 20 in PBS. Stock solutions of beads (2×10^6 beads/mL) including these blocking agents were allowed to incubate for at least 24h before use. Shortly before use beads were added to cells and mixed gently by pipette. Lysates were then produced using SAW from solutions of PBS containing:

- BE cells (1×10^6 cells/mL) only
- BE cells (1×10^6 cells/mL) plus 10µm beads (1×10^6 beads/mL)
- BE cells (1×10^6 cells/mL) plus 10µm beads (1×10^6 beads/mL) with 4% BSA blocking
- BE cells (1×10^6 cells/mL) plus 10µm beads (1×10^6 beads/mL) with 0.05% Tween 20 blocking

As a control to compare the yield of p53 protein in SAW lysates, a stock of lysate was produced from a solution containing 2×10^6 cells/mL mixed with an equal volume of detergent lysis buffer. Before introducing lysates into the MAC chip, a detection antibody solution was added 1:1 to the lysates so that the final test solution contains 0.5× concentrated lysate plus 0.25µg mL^{-1} anti-p53 Alexa-Fluor 488-labelled detection antibody in 2% PBSA.

MAC chips were prepared as above and each test solution was flowed into separate lanes of the MAC chip (4 SAW test solutions plus detergent lysis control). After 5µL of each solution was perfused at a rate of 5µL min^{-1} image acquisition was started. The number of single molecules bound to the spots after 90min was counted and results are shown in **figure 5** along with representative raw images of the antibody spots.

For the detection of p53 protein in lysate produced from BE cells, SAW lysis is ~9 – 13% as efficient as conventional detergent-based lysis using the methods presented here. For sample droplets containing cells alone, SAW lysis efficiency is 9.8 ± 0.3%, where the uncertainty is quoted as the standard error. The addition of unblocked beads to the sample droplet does not improve efficiency, 9.2 ± 0.6%, and may be acting to slightly reduce it. It is possible that any enhancement in the disruption of cells is counteracted by non-specific binding of proteins to the surface of the beads. Similarly, beads blocked with Tween 20 do not enhance SAW lysis efficiency (9.9 ± 0.7%) although there may be indication of a mild effect of blocking when compared to beads that are not blocked. The addition of beads blocked with 4% BSA resulted in a 2-3% enhancement in efficiency to 12.9 ± 0.7%. Due to its proficiency in blocking the microfluidic channels and capture antibody spots in the MAC chip, the final concentration of 2% BSA in the droplet was adequate in both blocking the surface of the silicon superstrate and the beads.

In BE cells, p53 protein has been shown to accumulate in the nucleus. However, judging by the extent of nuclear disruption observed in **figure 4e,** we would expect a greater efficiency than that suggested by the readout of the MAC chip. This may indicate that despite a near-complete disruption of cells there are additional sources of protein loss associated with chemical-free SAW lysis which limit overall efficiency.

Upon disruption, intracellular proteases will be released and potentially reduce protein yield. It is possible that the enhancement observed with beads blocked with 4% BSA is due to the BSA, which remains in solution unbound to beads, engaging liberated proteases in the droplet during and after lysis. Their proteolytic activity is temperature dependent and so should be significantly inhibited when SAW lysate is put on ice.

Other potential loss mechanisms are the denaturation of p53 proteins due to heat, adsorption to the air/water interface of the droplet or mechanical stress within the vortexing droplet. The dissipation of acoustic energy will generate heat. Although when tested under similar conditions the temperature of 20µL

droplets rose from room temperature to 38°C during SAW lysis. The average thermal energy per molecule is approximately $k_BT = 4.3 \times 10^{-21}$ J, where k_B is the Boltzmann constant. The shear stress has been previously estimated to be ~85 Pa within the droplet under conditions used for lysis. According to Walstra, the total deformation energy applied to a molecule is the shear stress multiplied by the molecular volume.[37] Erickson provides the following relationship to estimate the volume occupied by a protein from its mass M, V (nm^3) = 1.212×10^{-3} (nm^3/Da) × M (Da).[38] Consequently, the deformation energy applied to a p53 protein within the droplets during lysis may be estimated to be $\sim 4.5 \times 10^{-24}$ J. The stability of the core domain of wild-type p53 is 5.2×10^{-20} J/molecule and 2.1×10^{-20} J/molecule at 25°C and 37°C, respectively.[39] The deformation energy due to shear stress is therefore much smaller than would be needed to affect the protein and implies a shear stress in excess of 4×10^5 Pa would be required to denature p53. The solution of cells and beads is kept on ice prior to SAW so it is unlikely that the droplet reaches 38°C as in previous experiments. Moreover, 99% of the wild-type protein would remain folded even at 37°C.[40] Therefore, it seems unlikely that heat or mechanical stress within the droplet under the SAW lysis conditions used here would lead to any significant amount of protein loss.

Proteins are known to adsorb from solution onto surfaces which includes the air-water interface of the SAW lysis droplet. At the droplet surface there is a reduction in surface free energy of *ca.* 20 mJ m^{-2}.[37,41] It is assumed that the volume of the p53 protein estimated above refers to a sphere[38] and that the protein contacts the air-water interface with an area equal to that of the great circle of the sphere. Under these assumptions, the free energy decrease is $\sim 3.41 \times 10^{-19}$ J upon adsorption of a p53 protein to the air-water interface. When compared to the stability of the core domain of wild-type p53 (see above), there is sufficient free energy to induce a change in conformation.

Without agitation the transport of proteins to the interface would be diffusion limited. In the droplets, the mixing effect of the vortex will act to increase the rate of mass transport. However, it is not known what proportion of p53 proteins will adsorb to the air-water interface from solution or what proportion denatures during adsorption.

Although several mechanisms are potentially able to limit the overall efficiency, the most predominant sources of p53 protein loss are likely to be the degradation of protein due to the release of intracellular proteases or their adsorption to the air-water interface.

In **figure 5b** images of typical spots are shown along with average single molecule counts. The spot is congested with counts of $\sim 10^5$ single molecules when incubated with lysates produced by SAW. Counts are $\sim 10^3$ times that of the limit of detection as determined by the amount of NSB to the capture spot (see **figure 2c**). It is possible to detect p53 protein in samples with a much lower total expression of protein with the limit of detection in the chambers as determined by NSB to be 113 ± 36 single molecule counts.

The methods presented here have potential to be developed into a sensitive point-of-care device for the detection of aberrant p53 function in breast cancer patients. Nuclear localisation of p53 in response to DNA damage is essential for its tumour suppressor function. Aberrant cytoplasmic sequestration in response to DNA damage in such tumours is associated with poor response to chemotherapy.[30] For instance, one would utilise the tuneable mechanism of SAW lysis to fully or partially disrupt cells in a fine needle aspirate from a breast tumour to determine the tumours phenotype in this regard.

CONCLUSIONS

We have shown that SAW lysis is capable of completely or partially disrupting cells from a human cancer cell line as observed using fluorescence microscopy.

We demonstrate the combination of SAW to produce cell lysates and the MAC chip to detect the concentration of a specific protein within the complex mixture of a crude lysate. However, there exist several mechanisms leading to a reduction in the yield of p53 protein and the overall efficiency of the SAW lysis method in comparison to detergent-based lysis.

AUTHOR INFORMATION

Corresponding Authors

* ali.salehi-reyhani@imperial.ac.uk
* jon.cooper@glasgow.ac.uk
* d.klug@imperial.ac.uk

Author Contributions

† These authors contributed equally.

Notes

The authors declare no competing financial interest.

ACKNOWLEDGMENT

This work was supported by the Single Cell Proteomics Project at the Institute of Chemical Biology and the Proxomics Project, funded by the UK Engineering and Physical Sciences Research Council (EP/C54269X/1 and EP/I017887/1) and the Human Frontier Science Program under grant RGP0061/2011. JR acknowledges a Lord Kelvin and Adam Smith Fellowship from the University of Glasgow. JC acknowledges an EPSRC fellowship (EP/K027611/1) and an ERC Advanced Investigator Award. We thank the James Watt Nanofabrication Centre for their assistance with device fabrication.

REFERENCES

(1) Ullal, A. V; Peterson, V.; Agasti, S. S.; Tuang, S.; Juric, D.; Castro, C. M.; Weissleder, R. *Sci. Transl. Med.* **2014**, *6*, 219ra9.
(2) Liu, J.; Cooks, R. G.; Ouyang, Z. *Anal. Chem.* **2011**, *83*, 9221–9225.
(3) Balog, J.; Sasi-Szabó, L.; Kinross, J.; Lewis, M. R.; Muirhead, L. J.; Veselkov, K.; Mirnezami, R.; Dezső, B.; Damjanovich, L.; Darzi, A.; Nicholson, J. K.; Takáts, Z. *Sci. Transl. Med.* **2013**, *5*, 194ra93.
(4) Ding, X.; Li, P.; Lin, S.-C. S.; Stratton, Z. S.; Nama, N.; Guo, F.; Slotcavage, D.; Mao, X.; Shi, J.; Costanzo, F.; Huang, T. J. *Lab Chip* **2013**, *13*, 3626–3649.
(5) Länge, K.; Rapp, B. E.; Rapp, M. *Anal. Bioanal. Chem.* **2008**, *391*, 1509–1519.
(6) Destgeer, G.; Im, S.; Hang Ha, B.; Ho Jung, J.; Ahmad Ansari, M.; Jin Sung, H. *Appl. Phys. Lett.* **2014**, *104*, 023506.
(7) Reboud, J.; Auchinvole, C.; Syme, C. D.; Wilson, R.; Cooper, J. M. *Chem. Commun. (Camb).* **2013**, *49*, 2918–2920.
(8) Shilton, R. J.; Glass, N. R.; Chan, P.; Yeo, L. Y.; Friend, J. R. *Appl. Phys. Lett.* **2011**, *98*, 254103.
(9) Rogers, P. R.; Friend, J. R.; Yeo, L. Y. *Lab Chip* **2010**, *10*, 2979–2985.
(10) Bourquin, Y.; Wilson, R.; Zhang, Y.; Reboud, J.; Cooper, J. M. *Adv. Mater.* **2011**, *23*, 1458–1462.
(11) Schmid, L.; Weitz, D. A.; Franke, T. *Lab Chip* **2014**.

(12) Hartmann, A.; Stamp, M.; Kmeth, R.; Buchegger, S.; Stritzker, B.; Saldamli, B.; Burgkart, R.; Schneider, M. F.; Wixforth, A. *Lab Chip* **2014**, *14*, 542–546.

(13) Sivanantha, N.; Ma, C.; Collins, D. J.; Sesen, M.; Brenker, J.; Coppel, R. L.; Neild, A.; Alan, T. *Appl. Phys. Lett.* **2014**, *105*, 103704.

(14) Lyford, T. J.; Millard, P. J.; da Cunha, M. P. In *2012 IEEE International Ultrasonics Symposium*; IEEE, 2012; pp. 1216–1219.

(15) Reboud, J.; Bourquin, Y.; Wilson, R.; Pall, G. S.; Jiwaji, M.; Pitt, A. R.; Graham, A.; Waters, A. P.; Cooper, J. M. *Proc. Natl. Acad. Sci. U. S. A.* **2012**, *109*, 15162–15167.

(16) Taylor, M. T.; Belgrader, P.; Furman, B. J.; Pourahmadi, F.; Kovacs, G. T. A.; Northrup, M. A. *Anal. Chem.* **2001**, *73*, 492–496.

(17) Rezk, A. R.; Friend, J. R.; Yeo, L. Y. *Lab Chip* **2014**, *14*, 1802–1805.

(18) Taniguchi, Y.; Choi, P. J.; Li, G.-W.; Chen, H.; Babu, M.; Hearn, J.; Emili, A.; Xie, X. S. *Science* **2010**, *329*, 533–538.

(19) Newman, J. R. S.; Ghaemmaghami, S.; Ihmels, J.; Breslow, D. K.; Noble, M.; DeRisi, J. L.; Weissman, J. S. *Nature* **2006**, *441*, 840–846.

(20) Salehi-Reyhani, A.; Kaplinsky, J.; Burgin, E.; Novakova, M.; DeMello, A. J.; Templer, R. H.; Parker, P.; Neil, M. A. A.; Ces, O.; French, P.; Willison, K. R.; Klug, D. *Lab Chip* **2011**, *11*, 1256–1261.

(21) Hughes, A. J.; Spelke, D. P.; Xu, Z.; Kang, C.-C.; Schaffer, D. V; Herr, A. E. *Nat. Methods* **2014**, *11*, 749–755.

(22) Shi, Q.; Qin, L.; Wei, W.; Geng, F.; Fan, R.; Shin, Y. S.; Guo, D.; Hood, L.; Mischel, P. S.; Heath, J. R. *Proc. Natl. Acad. Sci. U. S. A.* **2012**, *109*, 419–424.

(23) Burgin, E.; Salehi-Reyhani, A.; Barclay, M.; Brown, A.; Kaplinsky, J.; Novakova, M.; Neil, M. A. A.; Ces, O.; Willison, K. R.; Klug, D. R. *Analyst* **2014**, *139*, 3235–3244.

(24) Salehi-Reyhani, A.; Sharma, S.; Burgin, E.; Barclay, M.; Cass, A.; Neil, M. A. A.; Ces, O.; Willison, K. R.; Klug, D. R. *Lab Chip* **2013**, *13*, 2066–2074.

(25) Greenbaum, A.; Luo, W.; Su, T.-W.; Göröcs, Z.; Xue, L.; Isikman, S. O.; Coskun, A. F.; Mudanyali, O.; Ozcan, A. *Nat. Methods* **2012**, *9*, 889–895.

(26) Zhu, H.; Yaglidere, O.; Su, T.-W.; Tseng, D.; Ozcan, A. *Lab Chip* **2011**, *11*, 315–322.

(27) Ramachandran, S.; Cohen, D. A.; Quist, A. P.; Lal, R. *Sci. Rep.* **2013**, *3*, 2133.

(28) Schindelin, J.; Arganda-Carreras, I.; Frise, E.; Kaynig, V.; Longair, M.; Pietzsch, T.; Preibisch, S.; Rueden, C.; Saalfeld, S.; Schmid, B.; Tinevez, J.-Y.; White, D. J.; Hartenstein, V.; Eliceiri, K.; Tomancak, P.; Cardona, A. *Nat. Methods* **2012**, *9*, 676–682.

(29) Stadler, C.; Skogs, M.; Brismar, H.; Uhlén, M.; Lundberg, E. *J. Proteomics* **2010**, *73*, 1067–1078.

(30) O'Brate, A.; Giannakakou, P. *Drug Resist. Updat.* **2003**, *6*, 313–322.

(31) Batchelor, E.; Mock, C. S.; Bhan, I.; Loewer, A.; Lahav, G. *Mol. Cell* **2008**, *30*, 277–289.

(32) Bode, A. M.; Dong, Z. *Nat. Rev. Cancer* **2004**, *4*, 793–805.

(33) Yoon, S. H.; Huang, Y.; Edgar, J. S.; Ting, Y. S.; Heron, S. R.; Kao, Y.; Li, Y.; Masselon, C. D.; Ernst, R. K.; Goodlett, D. R. *Anal. Chem.* **2012**, *84*, 6530–6537.

(34) Bryan, A. K.; Hecht, V. C.; Shen, W.; Payer, K.; Grover, W. H.; Manalis, S. R. *Lab Chip* **2014**, *14*, 569–576.

(35) Patton, W. F. *J. Chromatogr. B Biomed. Sci. Appl.* **1999**, *722*, 203–223.

(36) Rosner, M.; Schipany, K.; Hengstschläger, M. *Nat. Protoc.* **2013**, *8*, 602–626.

(37) Dickinson, E.; Miller, R.; Walstra, P. *Food Colloids*; Dickinson, E.; Miller, R., Eds.; Royal Society of Chemistry: Cambridge, 2001.

(38) Erickson, H. P. *Biol. Proced. Online* **2009**, *11*, 32–51.

(39) Bullock, A. N.; Henckel, J.; DeDecker, B. S.; Johnson, C. M.; Nikolova, P. V.; Proctor, M. R.; Lane, D. P.; Fersht, A. R. *Proc. Natl. Acad. Sci.* **1997**, *94*, 14338–14342.

(40) Bullock, A. N.; Fersht, A. R. *Nat. Rev. Cancer* **2001**, *1*, 68–76.

(41) Walstra, P.; De Roos, A. L. *Food Rev. Int.* **1993**, *9*, 503–525.

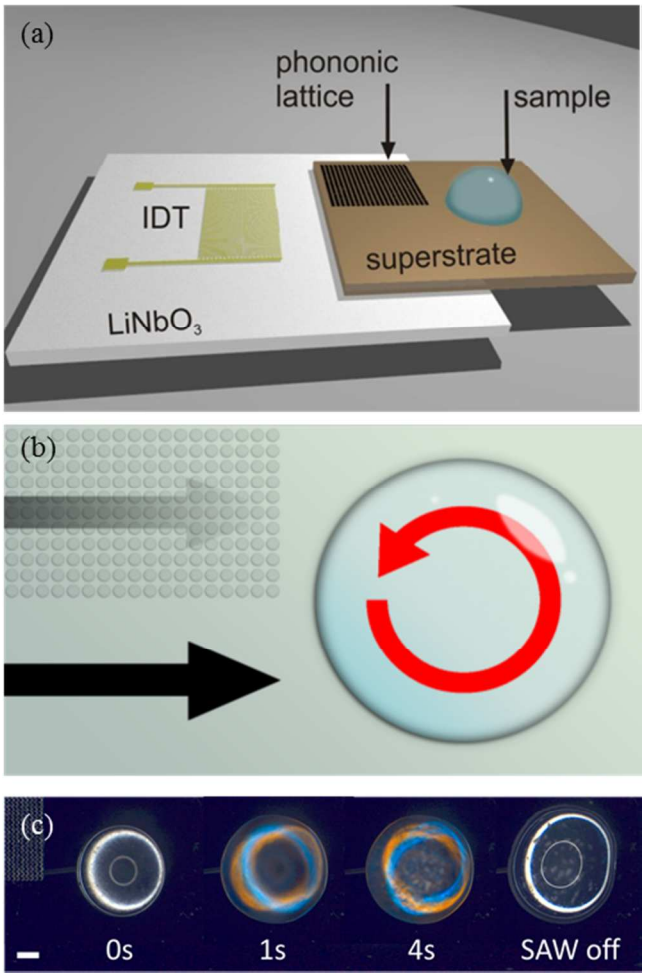

Figure 1. The Surface Acoustic Wave (SAW) platform is used to lyse cells. a) Device architecture showing the IDT used to gener ate the SAW on the $LiNbO_3$ piezoelectric wafer. The SAW is coupled into a phononic superstrate. A 20µL droplet containing the cell suspension is deposited in the position shown. b) The phononic lattice absorbs SAWs in a frequency dependent manner. At ~10MHz, propagation is hindered in region of the lattice whereas it is unhindered in the adjacent region. This acts to create a rotational movement within the droplet and results in shear flows that contribute to the disruption of the cell membrane. c) The sequence of images shows a droplet of cells undergoing SAW induced mechanical lysis. The droplet containing cells has a cloudy appearance which is observed to become largely clear upon successful lysis of cells. Note that the coloured rings ob served in part of the image sequence are an optical effect of the stereo microscope used to observe lysis. Scale bar 1mm.

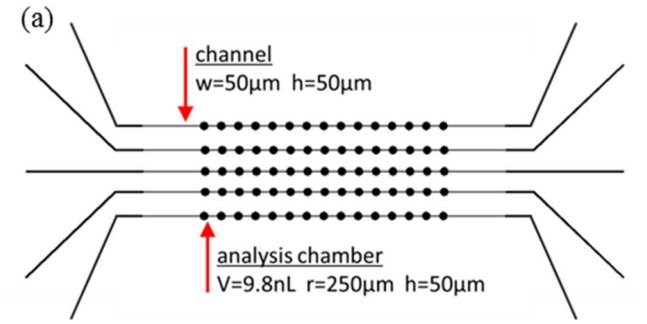

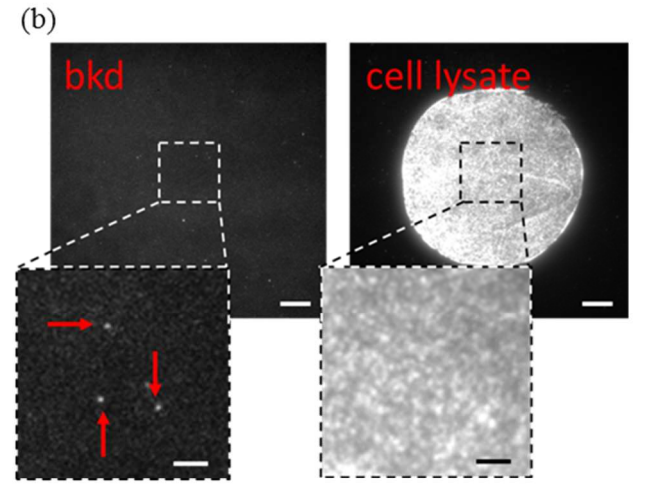

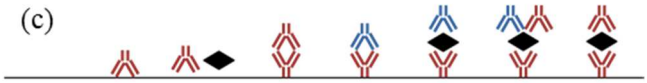

Primary AB	None	None	P53 antibody	P53 antibody	P53 antibody	P53 antibody	P53 antibody
Detection AB	P53 antibody	P53 antibody	P53 antibody	MDM2 antibody	MDM2 antibody	P53 antibody & MDM2 antibody	P53 antibody
Antigen	None	BE lysate	None	None	BE lysate	BE lysate	BE lysate
Count	129 ± 10	163 ± 43	113 ± 36	359 ± 87	451 ± 130	$> 10^6$	$>10^6$

Figure 2. The Microfluidic Antibody Capture platform is used to assess SAW lysis performance. a) Schematic of the 5 lane MAC chip with 15 analysis chambers per lane used to determine the amount of p53 protein in the SAW lysates. Each of the 50 analysis chambers contains a single antibody spot printed onto a coverslip which forms the floor of the PDMS-based chip. Each lane is separately addressed so that 5 separate lysate solutions may be assessed. b) Typical raw images showing the non-specific background (bkd) of the detection antibody and the specific binding (cell lysate) of p53 protein captured within each chamber from BE cell lysate produced using detergents (1×10^6 cells mL^{-1}). The red arrows in the background inset highlight what are counted as single molecules. When the spot captures a large number of single molecules they overlap and are individually indistinguishable as shown in the cell lysate inset. The number of proteins captured is then calculated by dividing the antibody spot intensity by the known average intensity of the single molecules. Scale bars 15µm (inset 5µm). c) Summary of control experiments to determine the performance of the MAC chip assay to detect p53 protein in lysate.

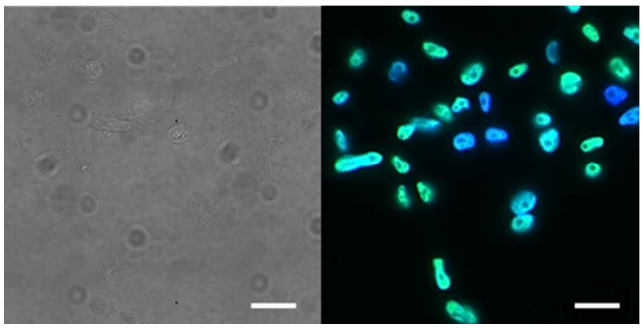

Figure 3. Immunofluorescence images of BE cells attached to coverslips. Representative composite image showing that p53 (green) is expressed in these cells and is accumulated in the nucleus (blue; Hoechst 33342). Scale bars 30µm.

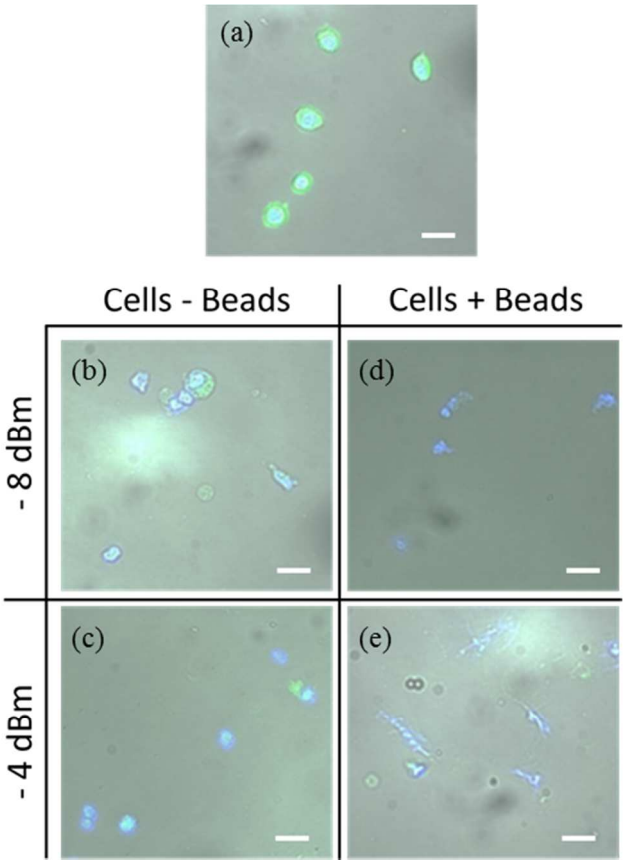

Figure 4. Representative images showing the extent of cellular disruption for different SAW lysis variables. Prior to lysis, BE cells are stained with Calcein AM (green, FITC channel) and Hoechst 33342 (blue, DAPI channel) to highlight the cytoplasm and the nucleus, respectively. Lysate is briefly centrifuged to remove beads. a) The appearance of cells prior to SAW actuation. b) Cells are ruptured but a few cell cytoplasms and most nuclei remain intact when -8dBM power is applied. c) Increasing power to -4dBm results improves disruption but little change is observed to cell nuclei. d) The addition of beads improves the efficiency and extent to which cells are lysed. At -8dBm all cell membranes are disrupted. Nuclei are observed to remain intact but with a shrivelled appearance. e) Increasing power to -4dBm with beads results in both the disruption of cell cytoplasms and nuclei. Scale bars 10µm.

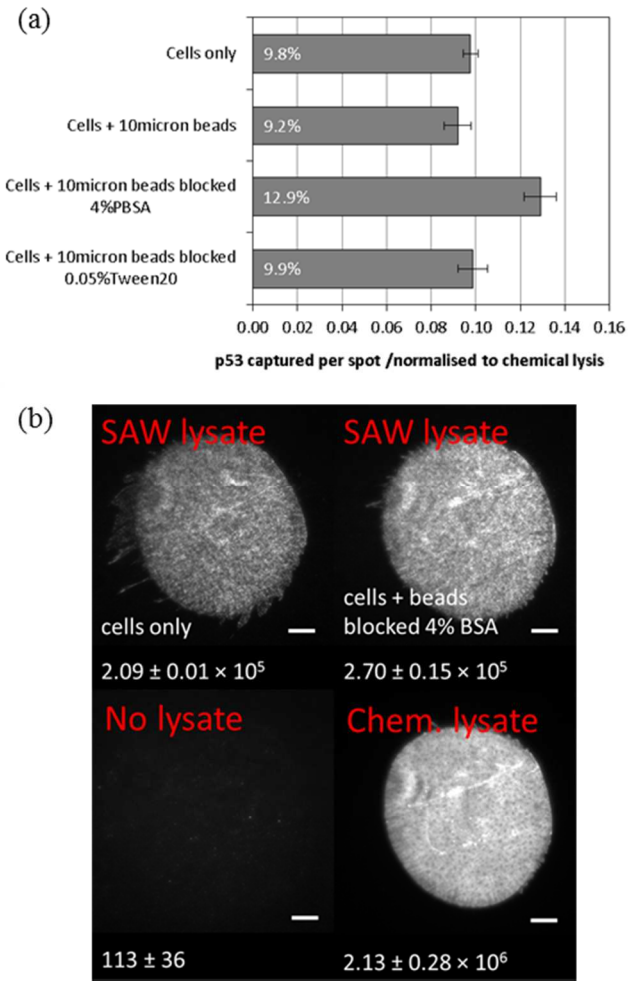

Figure 5. Protein yield in lysates produced using SAW as assessed by the MAC chip. The amount of p53 captured by the spots is normalised to that from lysate produced using detergent. a) On average SAW lysis is ~9-13% as efficient as detergent-based chemical lysis with a maximum of 12.9 ± 0.7% measured when using 10µm beads blocked with 4% BSA. Error bars represent the standard error of the mean of 3 separate runs using the MAC chip. b) Representative images of capture antibody spots at equilibrium after incubation with lysates. For comparison, brightness and contrast of spot images are adjusted relative to SAW lysate spots with 'cells only' lysate. However, the brightness of the chemical lysate spot is reduced here to avoid saturation. Scale bars 15µm.

Graphic entry for the Table of Contents (TOC)